

Correlations Between Lag, Luminosity, and Duration in Gamma-ray Burst Pulses

Jon Hakkila¹, Timothy W. Giblin², Jay P. Norris³,
P. Chris Fragile¹, and Jerry T. Bonnell⁴

¹*Dept. Physics and Astronomy, The College of Charleston, Charleston, SC 29424-0001*

²*Dept. Physics and Astronomy, The University of North Carolina, Asheville, NC*

³*Space Science Division, NASA/Ames Research Center, Moffett Field, CA*

⁴*UMCP/CRESST/GSFC - Greenbelt, MD*

hakkilaj@cofc.edu

ABSTRACT

We derive a new peak lag vs. peak luminosity relation in gamma-ray burst (GRB) pulses. We demonstrate conclusively that GRB spectral lags are *pulse* rather than *burst* properties and show how the lag vs. luminosity relation determined from CCF measurements of burst properties is essentially just a rough measure of this newly derived relation for individual pulses. We further show that most GRB pulses have correlated properties: short-lag pulses have shorter durations, are more luminous, and are harder within a burst than long-lag pulses. We also uncover a new pulse duration vs. pulse peak luminosity relation, and indicate that long-lag pulses often precede short-lag pulses. Although most pulse behaviors are supportive of internal shocks (including long-lag pulses), we identify some pulse shapes that could result from external shocks.

Subject headings: gamma-ray bursts

1. Introduction

Gamma-ray burst (GRB) prompt emission has remained enigmatic over the years, even as our understanding of afterglow physics has evolved. Time intervals containing flux increases (*pulses*) exhibit some general behaviors, including (1) longer decay than rise rates, (2) hard-to-soft spectral evolution, and (3) broadening at lower energies (e.g. Norris et al. (1996); Ryde (2005)).

The *spectral lag* is the delay between photons observed in a high-energy bandpass relative to a lower-energy one; it is primarily obtained through application of the cross-correlation

function (CCF; Band (1997)). In general, lag is an indicator of both GRB peak luminosity (e.g. Norris et al. (2000); Norris (2002)) and time history morphology (Hakkila et al. 2007), with short-lag, variable bursts having greater luminosities than long-lag, smooth bursts.

The short durations, spectral evolution, and short interpulse durations of most GRB pulses suggest that they originate from *internal* shocks in relativistic winds (e.g. Daigne & Mochkovitch (1998); Ramirez-Ruiz & Fenimore (2000); Nakar & Piran (2002)). However, some bursts exhibit a soft component indicative of afterglow onset (e.g. Giblin et al. (2002)) which could be interpreted as the initial *external* shock. Prompt afterglow emission begins preferentially towards the end of the burst or even after the GRB ends, as suggested by several x-ray afterglows observed by BeppoSAX (Costa 2000) and Swift (Panaitescu 2007), but it can also appear at a time early enough to overlap the short-timescale emission (as observed in GRB 980923 (Giblin et al. 1999)). In addition, co-adding fluxes of many BATSE GRBs has led to observation of extended soft gamma-ray emission possibly indicating the same phenomenon (Connaughton 2002).

Internal and external shocks have both been predicted theoretically (e.g. Sari & Piran (1999)), and it has been suggested that both shock types are observed within quiescent BATSE GRBs 960530 and 980125 (Hakkila & Giblin 2004). *Quiescent* GRBs release their prompt emission in more than one distinct *emission episode* (each episode contains one to many overlapping pulses). Although the pre-quiescent emission episodes of these two GRBs satisfy the standard internal shock paradigm, the long episodic lags, smooth morphologies, and soft spectral evolution of the later episodes are more consistent with external shocks, indirectly implying that the pulses comprising these episodes might also relate to specific types of shocks (however, see Chincarini et al. (2007)). Other observations support the idea that lag can vary within GRBs, and indirectly suggest that these variations are associated with pulses (e.g. Norris (2002); Ryde et al. (2005); Chen et al. (2005)). However, no study has yet isolated and delineated pulse spectral properties; to this end and to test the hypothesis that short- and long-lag pulses have different origins, we have set out to model pulses and study their spectral dependences.

2. Pulse Identification and Fitting Technique

We have developed a semi-automated pulse-identification and fitting routine using BATSE 64 ms data. The Bayesian Blocks (BB) routine (Scargle 1998) is applied to summed 4-channel data and identifies regions over which counts change significantly. Each BB potentially contains a pulse, and is fit using the pulse model of Norris et al. (2005):

$$I(t) = A\lambda \exp^{[-\tau_1/(t-t_s)-(t-t_s)/\tau_2]} \quad (1)$$

where t is time since trigger, A is the pulse amplitude, t_s is the pulse start time, τ_1 and τ_2 are characteristics of the pulse rise and pulse decay, and $\lambda = \exp [2(\tau_1/\tau_2)^{1/2}]$. Additionally, a two-parameter linear background model is assumed. Reasonable initial guesses are made using the starting and ending BB boundaries and the highest flux found in this BB. The non-linear least squares routine MPFIT (<http://idlastro.gsfc.nasa.gov/contents.html>) simultaneously fits all of the pulses and the background, iterating initial guesses to a convergent solution as characterized by χ^2 per degree of freedom. Statistically insignificant pulses are deselected from the initial pulse fit using a dual-timescale threshold (Hakkila et al. 2003) and Occam’s Razor. The dual-timescale threshold is chosen over a peak flux (favoring short, intense pulses) or fluence threshold (favoring long, low-intensity pulses) because it treats equally pulses peaking on short and long timescales. The reduced model is run again with fewer pulses until it converges and only pulses brighter than the dual-timescale threshold remain. The 4-channel pulse characteristics are used as starting points from which individual energy channel pulse characteristics are obtained. The process described above is repeated until convergent solutions are obtained for pulses in each energy channel.

Pulse peak lags are defined as the differences between the pulse peak times in different energy channels (pulse peak times are given by $\tau_{\text{peak}} = t_s + \sqrt{\tau_1\tau_2}$). Pulse peak lags can be obtained for any pulse between two energy channels, although we define the standard l_{pp} as that measured between energies of 100 to 300 keV (BATSE channel 3) and 25 to 50 keV (BATSE channel 1). Other measurable pulse properties include the pulse width $w = [9 + 12\sqrt{\tau_1/\tau_2}]^{1/2}$ and the pulse asymmetry $\kappa = w/(3 + 2\sqrt{\tau_1/\tau_2})$. These definitions are based on time intervals between intensities of Ae^{-3} , rather than of Ae^{-1} (Norris et al. 2005). We note that the *modeled* pulse duration definition of w is less susceptible to statistical variations near the beginning and end of the pulse than observationally-defined durations such as T_{90} .

Pulse parameter uncertainties are obtained using Monte Carlo analysis because Gaussian error assumptions (Norris et al. 2005) is not always valid for t_s , τ_1 , and τ_2 . These distributions often resemble lognormal or multi-modal distributions, and improperly-quoted uncertainties in these parameters often lead to overestimated uncertainties for pulse peak time amplitudes, durations, and asymmetries.

3. Analysis

Energy-dependent pulse properties are regularly identified and extracted using this technique, even though the pulse-finding technique is energy-independent. Multi-lag GRBs are apparently the norm for most Long GRBs. When the signal is strong enough that pulses

can be cleanly and unambiguously extracted, their characteristics are generally consistent across all energy channels (e.g. lags are observed across all energy channels in proportion to the energy channel separation). Within the limit of uncertainty, it appears that every pulse is characterized by its own lag. This is not to say that all pulses are clearly identified from one energy channel to another; there are fitting ambiguities caused by pulse evolution, pulse overlap, and low signal-to-noise (such as is found in BATSE channel 4). Additionally, it is difficult to uniquely fit many overlapping pulses because a pulse’s fitted signal-to-noise is not solely dependent on background; the flux of other pulses is “noise” to this fit.

We demonstrate results with the fit to GRB 950325a (BATSE trigger 3480), in which three overlapping pulses are observed with fairly high signal-to-noise in all four BATSE energy channels. Fitted channel 1 and channel 3 time histories are shown in Figure 1. The CCF burst lag $l_{pp} = 0.014s \pm 0.009$ (Hakkila et al. 2007). Some properties of the extracted pulses are listed in Table 1; these include the pulse fit parameters l_{pp} , w , and κ as well as CCF pulse lags. Pulse CCFs have been reconstructed from multichannel pulse parameters and the burst’s Poisson background. The greatest contribution to the CCF lag is found to come from the shortest-lag, highest-intensity pulses. In fact, the CCF lag appears to be insensitive to the presence of longer-lag pulses, which can appear at any time during a burst. The CCF and pulse peak lags occasionally disagree: the CCF lag of pulse 2 is demonstrably negative, even though the pulse has a moderately long pulse lag that is measured consistently across all four energy channels. We are currently exploring the effects of pulse shape on the CCF. The CCF of the original burst is essentially identical to that of the reconstructed burst, indicating that the long- and short-lag pulses have been combined to reproduce a good facsimile of the original short-lag GRB.

The sensitivity of the CCF to the shortest, brightest pulses provides an explanation for why Norris et al. (2000) finds different CCF lags when their burst data are confined to different intensity regimes via an apodization technique. Their removal of the low-intensity flux predominantly removes CCF contributions from the longest duration, longest-lag pulses, and improves the ability to measure the signal from the short-lag pulses.

3.1. Spectral-Dependent Pulse Properties

Although we are in the early stages of analyzing GRB pulse data, it is already apparent that the vast majority of GRB pulses have correlated spectral and temporal properties. Pulse lag, amplitude, duration, and hardness are linked; correlations between these behaviors lead us to believe that most GRB pulses represent a single physical phenomenon. Pulses exhibiting possible exceptions to these behaviors are those that cannot be appropriately fit

using these techniques. These pulses tend to fall into three categories: (1) pulses in crowded fields that cannot be unambiguously resolved (many have very short durations), (2) low signal-to-noise pulses that cannot be unambiguously resolved, and (3) bright yet uncommon pulses having shapes not adequately fitted by the four-parameter pulse model; when we are able to force a fit, we find these pulses to typically have short rise and very long decay times. We cannot ascertain if there are systematic biases in pulse sampling, because we cannot know the properties of pulses we cannot measure. However, we note that we preferentially cannot fit pulses in complex GRBs, as these bursts by definition have many overlapping pulses.

Two key correlations are identified in a sample of 24 pulses from 13 BATSE bursts (Hakkila et al. 2008): (1) *Pulse amplitude* (measured across BATSE’s four-channel energy range in units of counts sec^{-1}) *decreases with increasing lag* (a Spearman rank-order correlation test indicates a probability of only 2.4×10^{-8} that this correlation could occur randomly), and (2) *Pulse width w* (measured across BATSE’s four-channel energy range) *increases with increasing lag* (the Spearman rank-order probability is 1.7×10^{-7}). It is remarkable that these correlations are robust enough to be clearly identified in the observer’s rather than in the GRB rest frame; intrinsic pulse properties (e.g. jet properties) must be significantly larger than extrinsic effects (e.g. cosmological redshift and the inverse square law) for this to be true. Short-lag pulses are brighter and shorter than long-lag pulses; this appears to be true both within bursts and from one burst to another.

To clarify what these relationships mean, we fit pulses of BATSE bursts with known redshift; these GRBs originally defined the lag vs. peak luminosity relation (Norris et al. 2000). Some pulses in these GRBs cannot be fitted due to poor resolution and/or pulse overlap, so several complex GRBs have been limited to only one or two isolated pulses each. The resulting sample consists of 12 pulses in 7 bursts. Fitted peak fluxes have been re-calibrated on the 256 ms time scale so that the results can be compared to those of Norris et al. (2000). The pulse peak lag, pulse duration, and pulse intensity have been corrected to the GRB rest frame. The pulse characteristics are plotted in Figures 2 through 4. Also plotted are pulses from BATSE GRBs without known redshifts, assuming $z = 1$. These pulses demonstrate 1) the pervasiveness of the correlations, and 2) the strength of these intrinsic relationships relative to cosmological effects.

Figure 2 demonstrates the pulse peak luminosity L_{51} (the isotropic pulse peak luminosity L in units of $10^{51} \text{ erg s}^{-1}$) vs. the rest frame pulse peak lag l_0 (obtained by shifting l_{pp} into the rest frame); this is similar to the Norris et al. (2000) lag vs. peak luminosity diagram, except that it has been applied to *pulses* rather than to the bursts themselves. The best-fit functional form of this relation (excluding underluminous GRB 980425) is $\log(L_{51}) = A + B \log(l_0)$ (A is

in units of 10^{51} ergs s^{-1}). An anti-correlated relationship (correlation coefficient $R = -0.72$) is identified, with $A = 0.54 \pm 0.05$ and $B = -0.62 \pm 0.04$. The validity of this relation for pulses both within and across GRBs implies that the pulse peak lag vs. pulse peak luminosity relation is a fundamental one, while the CCF lag vs. peak luminosity relation is of secondary importance. In fact, the two relationships have different power-law indices, with the lag vs. peak luminosity relation’s power-law index being $B = -1.14 \pm 0.10$ (Norris et al. 2000). We have already demonstrated that the CCF lag is merely a rough measure of the narrowest pulse’s lag. Similarly, the peak flux is an overestimate of the narrowest pulse’s amplitude: peak flux results from summing fluxes from overlapping pulses, Poisson errors also make the measured peak fluxes larger than the modeled fluxes (the “Meegan Bias”).

Figure 3 plots the rest frame pulse duration (w_0 ; given in units of s) vs. pulse lag (l_0). Remarkably, the pulse duration vs. pulse lag correlation holds over four orders of magnitude in both duration and lag; even the underluminous GRB 980425 follows it. Its functional form in the GRB rest frame is taken as $\log(w_0) = C + D \log(l_0)$. From this small sample, the values of the coefficients are $C = 1.27 \pm 0.01$ s and $D = 0.85 \pm 0.01$, with $R = 0.95$.

The strong correlations in Figures 2 and 3 indicate that there must also be a *pulse width vs. pulse peak luminosity* relation. Figure 4 demonstrates this relation, which is more tightly defined ($R = -0.88$) than the pulse peak lag vs. pulse peak luminosity relation. Again, the exception to the rule is underluminous GRB 980425. The best-fit functional form of this relation in the GRB rest frame is $\log(L_{51}) = E + F \log(w_0)$, with $E = 1.53 \pm 0.02$ and $F = -0.85 \pm 0.02$ (E in units of 10^{51} ergs s^{-1}).

For GRBs with multiple fitted pulses, we also find that pulse spectral hardness (channel 3 pulse fluence divided by channel 1 pulse fluence) anti-correlates with pulse lag and duration, and correlates with pulse intensity. The same correlations are found in GRB 950325a, and imply that spectral evolution is present both across pulses and within them.

These results also allow new insights into the low peak luminosity of GRB 980425. This GRB’s single pulse is similar in lag and duration to the long-lag, long duration pulse of GRB 980703, implying a similar physical mechanism. Yet, GRB 980425 is still four orders of magnitude less luminous, similar to the underluminous, long-lag, long duration XRF 060218 (Liang et al. 2006). Although Gehrels et al. (2006) postulate a separate class of underluminous GRBs, pulse properties indicate that the low luminosity could still be due to a purely observational effect, such as large viewing angle relative to the jet (Salmonson 2001).

The apparently universal nature of most GRB pulses also explains why the CCF lag and the internal luminosity function power-law index (ILF) are excellent GRB time history

morphology indicators (Hakkila et al. 2007). CCF lags indicate the presence of short-lag pulses, while the ILF is a sensitive indicator of the number of pulses and of pulse shape.

The short durations of most GRB pulses, along with the similar behaviors seen in these pulses, argue that most pulses are related to internal shocks rather than external shocks. Since most pulses do not seem to have external shock characteristics, we look elsewhere to find these pulses; e.g. to pulses that cannot be fitted easily using the pulse model. Although we cannot say anything about faint or overlapping pulses, we suggest that pulses with short rise and very long decay times might represent external shocks capable of initiating afterglow. Such pulses appear to have short lags, although they are often fitted by two overlapping pulses; one short, large-amplitude, short-lag pulse and one long, small-amplitude, indeterminate-lag pulse. Suggestive of these pulse types is the extended tail in GRB 980923 (Giblin et al. 1999), thought to occur at the transition from prompt emission to afterglow. We are exploring this hypothesis.

4. Conclusions

Multi-lag GRBs are ubiquitous – this paper provides the first clear evidence in support of this statement. Each pulse appears to be characterized by its own lag; lag is a consequence of pulse evolution rather than a burst property. Burst peak luminosity and the CCF lag are not fundamental properties, but result from pulse combinations. Pulses are the basic, central building blocks of GRB prompt emission, and it is essential to our understanding of GRB physics that we properly catalog and characterize pulse properties.

Pulse lag, pulse luminosity, and pulse duration strongly correlate, implying that most GRB pulses have similar physical mechanisms; these are more consistent with internal than external shocks. Short pulses presumably indicate a collision of material at larger relative Lorentz factor than long pulses, and a large Lorentz factor requires a cleaner fireball with less baryonic matter. The fireball opacity dictates the emission timescale, so a clean, high-amplitude fireball should have a short decay and a short lag, while a dirty, low-amplitude fireball should produce a long decay and a long lag.

We are grateful to Rob Preece, Tom Lored, and Jeff Wragg for helpful discussions. The material presented here is based upon work supported by NASA under award No. GRNASNNX06AB43G and through the South Carolina NASA Space Grant program.

REFERENCES

- Band, D. L. 1997, *ApJ*, 486, 928
- Chen, L., Lou, Y.-Q., Wu, M., Qu, J.-L., Jia, S.-M., & Yang, X.-J. 2005, *ApJ*, 619, 983
- Chincarini, G., et al. 2007, *ApJ*, 671, 1903
- Connaughton, V. 2002, *ApJ*, 567, 1028
- Costa, E. 2000, *Gamma-ray Bursts*, 5th Huntsville Symposium, 526, 365
- Daigne, F., & Mochkovitch, R. 1998, *MNRAS*, 296, 275
- Gehrels, N., et al. 2006, *Nature*, 444, 1044
- Giblin, T. W., van Paradijs, J., Kouveliotou, C., Connaughton, V., Wijers, R. A. M. J., Briggs, M. S., Preece, R. D., & Fishman, G. J. 1999, *ApJ*, 524, L47
- Giblin, T. W., Connaughton, V., van Paradijs, J., Preece, R. D., Briggs, M. S., Kouveliotou, C., Wijers, R. A. M. J., & Fishman, G. J. 2002, *ApJ*, 570, 573
- Hakkila, J., Giblin, T. W., Roiger, R. J., Haglin, D. J., Paciesas, W. S., & Meegan, C. A. 2003, *ApJ*, 582, 320
- Hakkila, J., & Giblin, T. W. 2004, *ApJ*, 610, 361
- Hakkila, J., et al. 2007, *ApJS*, 169, 62
- Hakkila, J., et al. 2008, *Santa Fe Gamma-Ray Burst Conference*, in press.
- Liang, E.-W., Zhang, B.-B., Stamatikos, M., Zhang, B., Norris, J., Gehrels, N., Zhang, J., & Dai, Z. G. 2006, *ApJ*, 653, L81
- Nakar, E., & Piran, T. 2002, *MNRAS*, 331, 40
- Norris, J. P., Nemiroff, R. J., Bonnell, J. T., Scargle, J. D., Kouveliotou, C., Paciesas, W. S., Meegan, C. A., & Fishman, G. J. 1996, *ApJ*, 459, 393
- Norris, J. P., Marani, G. F., & Bonnell, J. T. 2000, *ApJ*, 534, 248
- Norris, J. P. 2002, *ApJ*, 579, 386
- Norris, J. P., Bonnell, J. T., Kazanas, D., Scargle, J. D., Hakkila, J., & Giblin, T. W. 2005, *ApJ*, 627, 324

- Norris, J. P. 2002, *ApJ*, 579, 386
- Panaitescu, A. 2007, *MNRAS*, 379, 331
- Ramirez-Ruiz, E., & Fenimore, E. E. 2000, *ApJ*, 539, 712
- Ramirez-Ruiz, E., & Merloni, A. 2001, *MNRAS*, 320, L25
- Ramirez-Ruiz, E., Merloni, A., & Rees, M. J. 2001, *MNRAS*, 324, 1147
- Ryde, F. 2005, *A&A*, 429, 869
- Ryde, F., Kocevski, D., Bagoly, Z., Ryde, N., & Mészáros, A. 2005, *A&A*, 432, 105
- Salmonson, J. D. 2001, *ApJ*, 546, L29
- Sari, R., & Piran, T. 1999, *ApJ*, 520, 641
- Scargle, J. D. 1998, *ApJ*, 504, 405

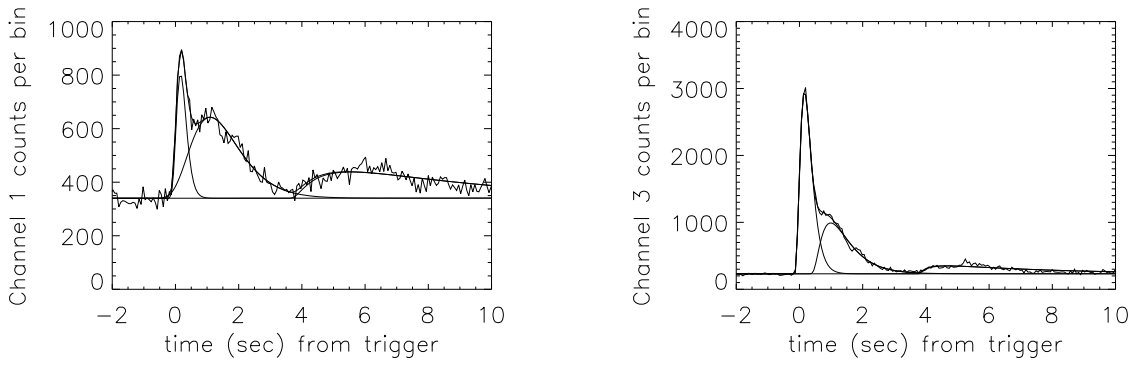


Fig. 1.— GRB 950325a pulse fits for BATSE channel 1 (first panel) and channel 3 (second panel).

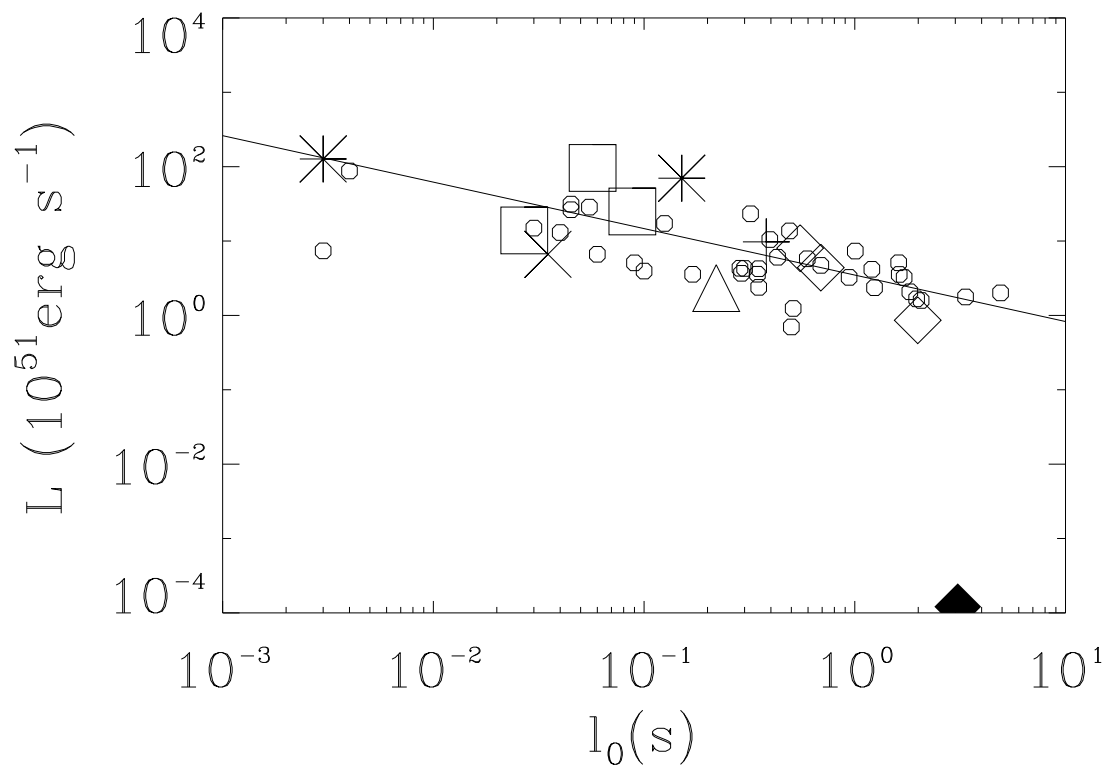


Fig. 2.— Isotropic pulse peak luminosity L vs. pulse peak lag (l_0) for fit pulses of BATSE GRBs having known luminosities. The sample consists of pulses from GRB 971214 (asterisk), GRB 980703 (open diamond), GRB 970508 (triangle), GRB 990510 (square), GRB 991216 (X), and GRB 990123 (plus), and the underluminous GRB 980425 (filled diamond). Symbol size denotes approximate uncertainty. Also plotted are 38 pulses from 22 BATSE GRBs without known redshifts (small circles); $z = 1$ is assumed.

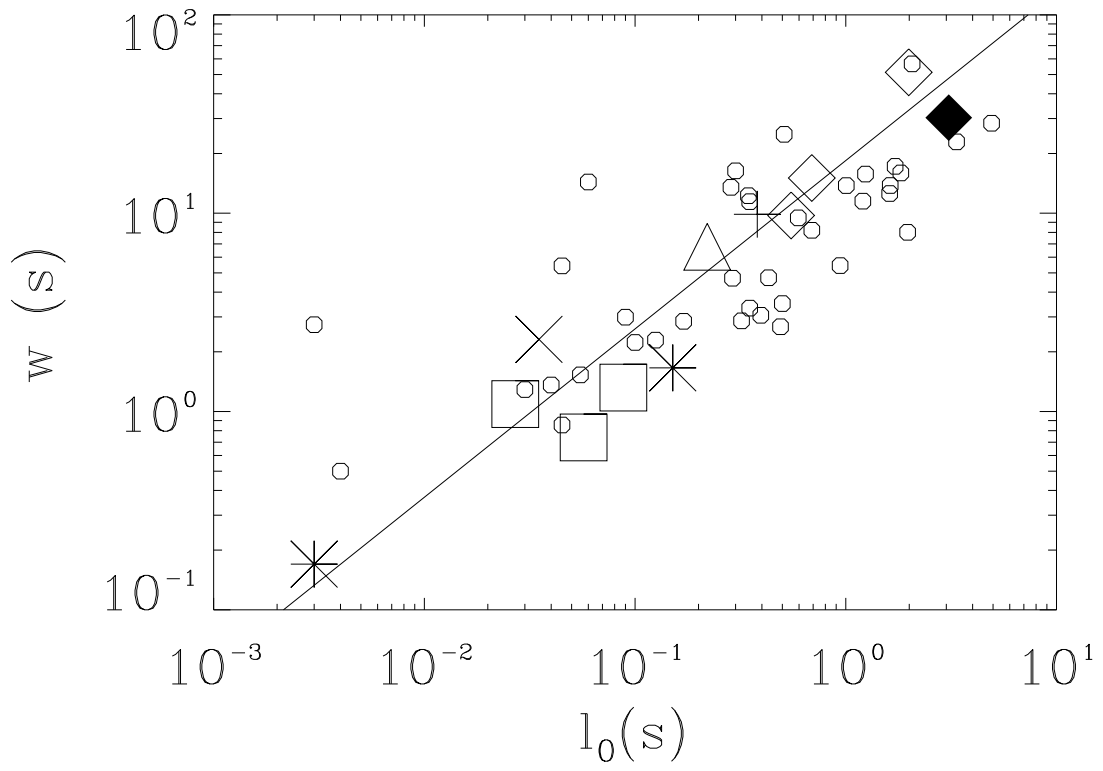


Fig. 3.— Pulse duration w vs. pulse peak lag (l_0) for pulses shown in Figure 2.

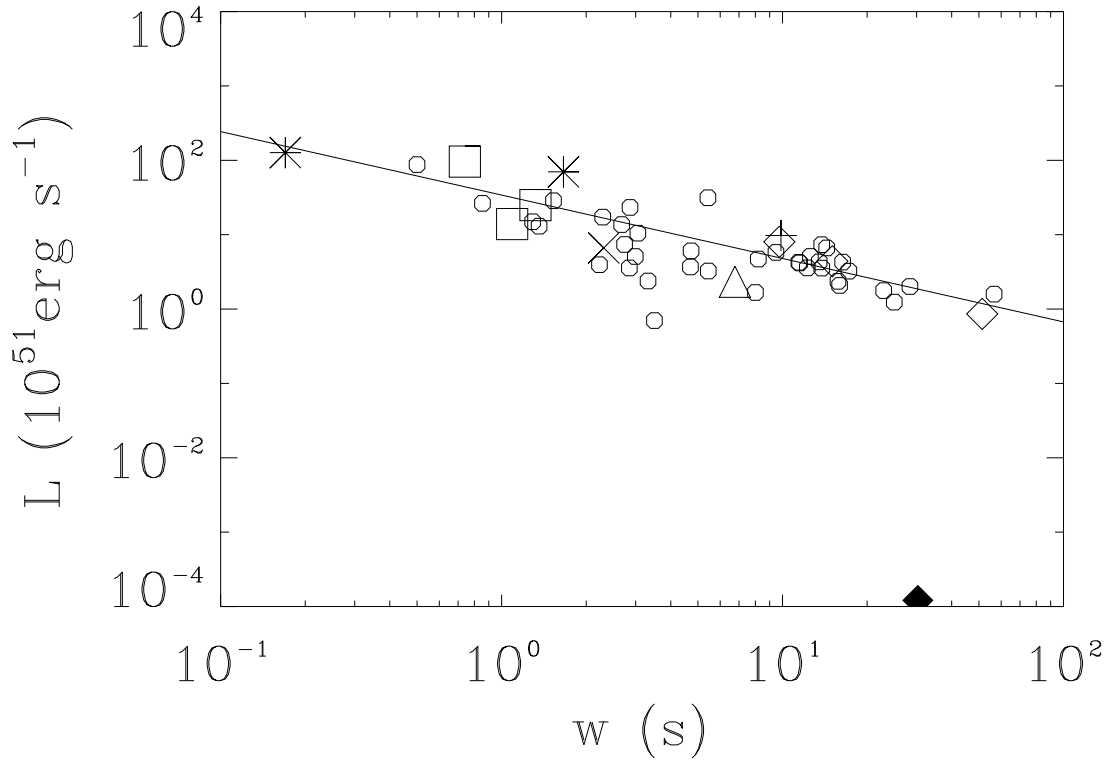


Fig. 4.— Pulse duration w vs. isotropic pulse peak luminosity L for pulses shown in Figures 2 and 3.

Table 1: Pulse Properties for GRB 950325a.

Pulse	peak (cts s ⁻¹)	$w(s)$	κ	$l_{pp}(s)$	$l_{CCF}(s)$
1	5112 ± 54	1.00 ± 0.08	0.76 ± 0.01	0.004 ± 0.009	0.006 ± 0.003
2	1669 ± 36	3.06 ± 0.10	0.87 ± 0.01	0.111 ± 0.045	-0.064 ± 0.020
3	354 ± 8	9.45 ± 0.52	0.93 ± 0.02	0.854 ± 0.150	0.414 ± 0.062